Repetition: Evaporation of Alloys

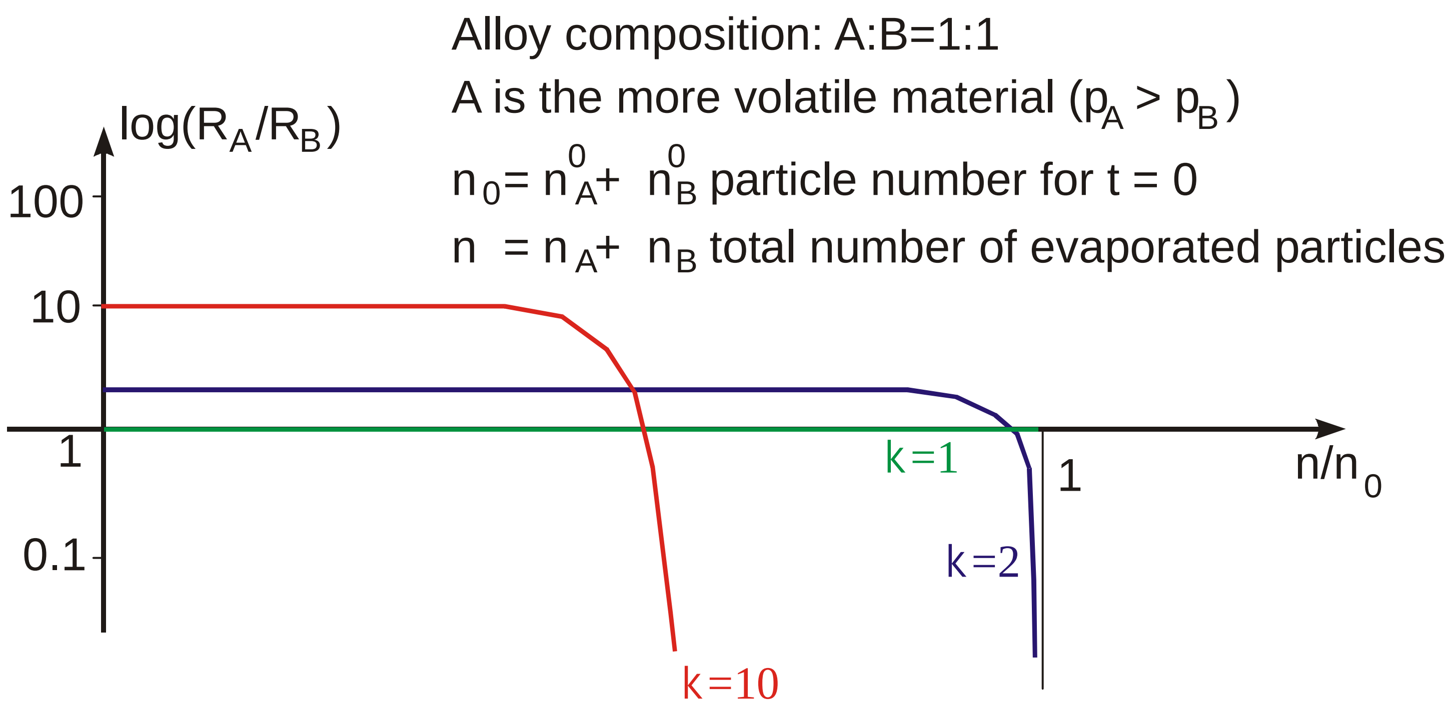

Evaporation of an alloy corresponds to a fractional destillation. The reason for this is the unhindered material transport within the source.

Repetition: Sputtering

Elementary Processes:

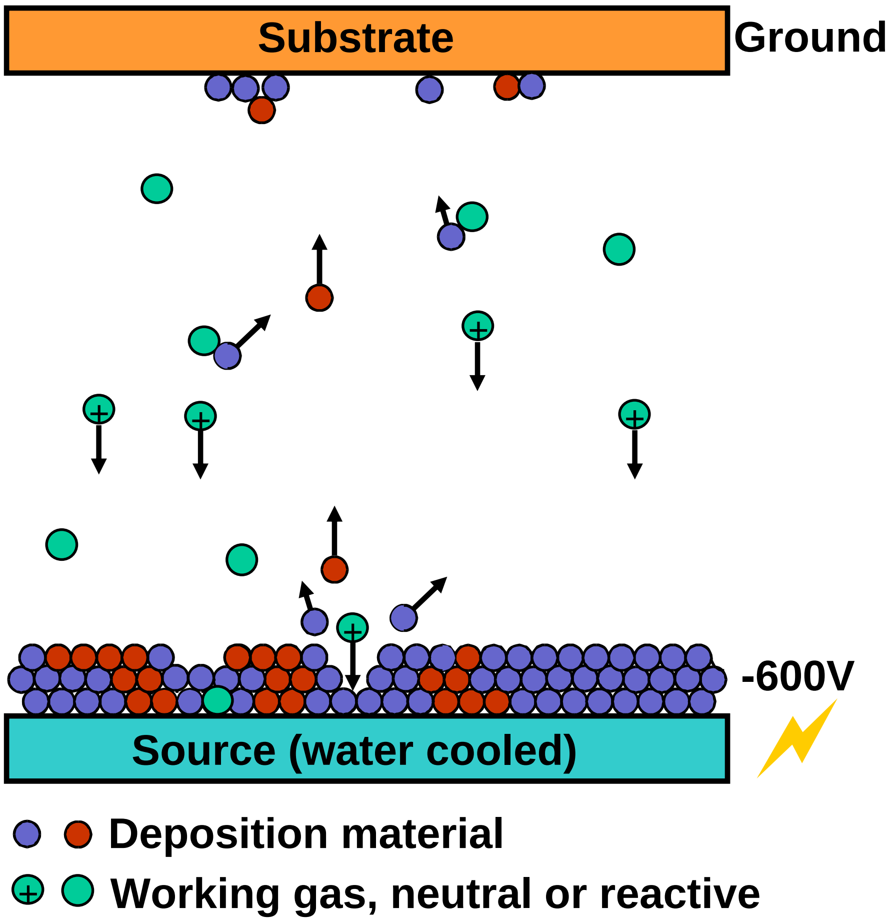

Characteristics:

- *Solid source, i. e. arbitrary source geometry*
- *Low deposition temperature*
- *High deposition rates can be reached*
- *Wide parameter field*
- *Coating composition = source composition*
- *Good coating adhesion*
- *Interesting film properties*

Repetition: Gas Discharge

Experimental set-up:

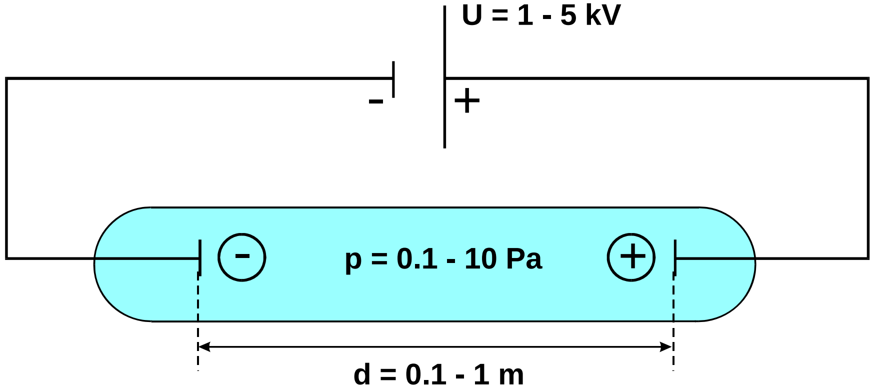

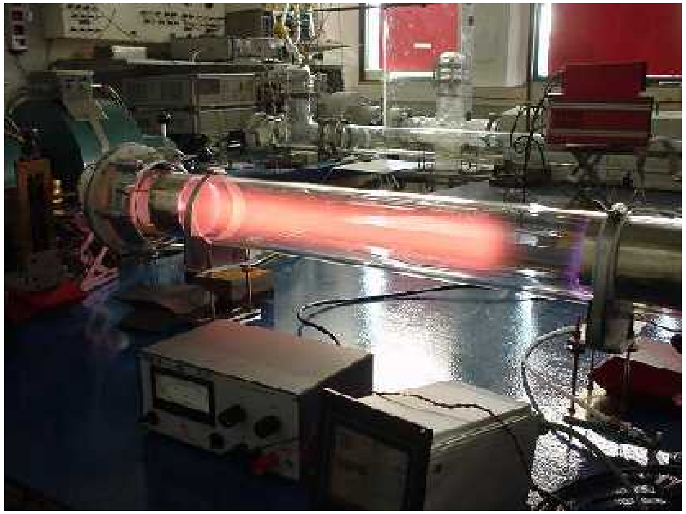

I/V characteristic:

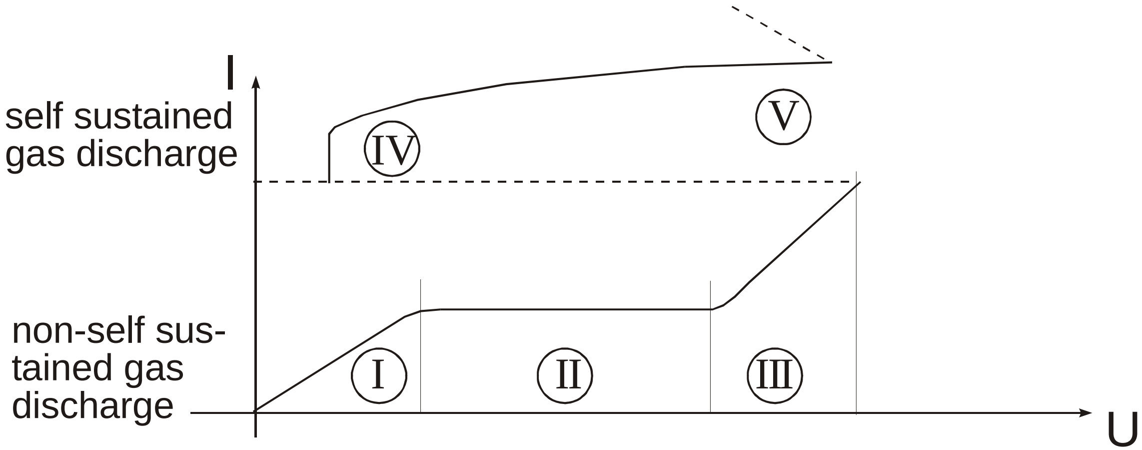

I: Ohmic behavior
II: Saturation region
III: collisional ionization/ Townsend-discharge
IV: normal glow
V: anormal glow secondary electron emission

Repetition: RF-Sputtering

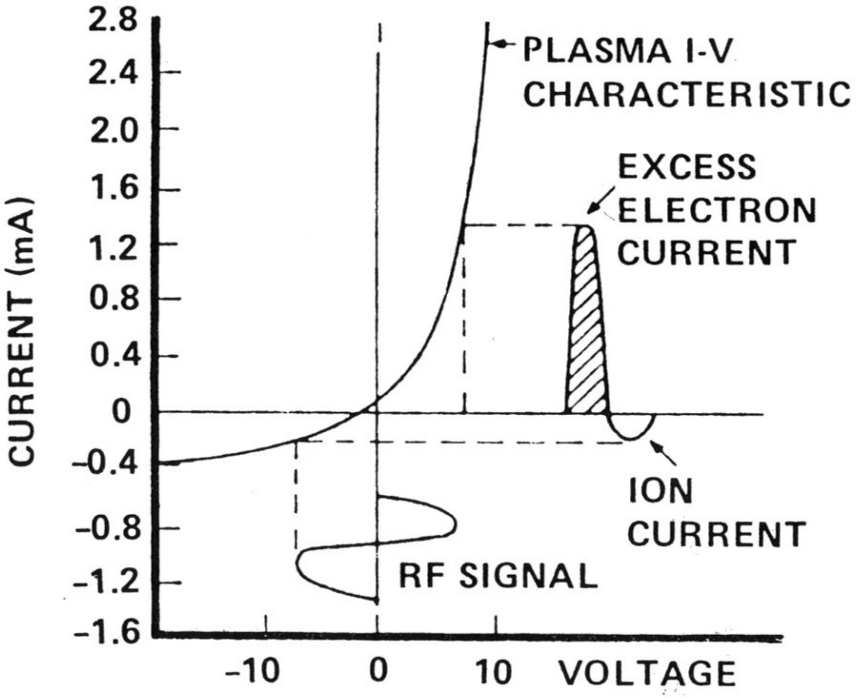

An excess electron current is generated by the higher electron mobility. It leads to a negative net voltage at the target, idependent wether the target is conductive or not.

Repetition: Magnetron-Sputtering

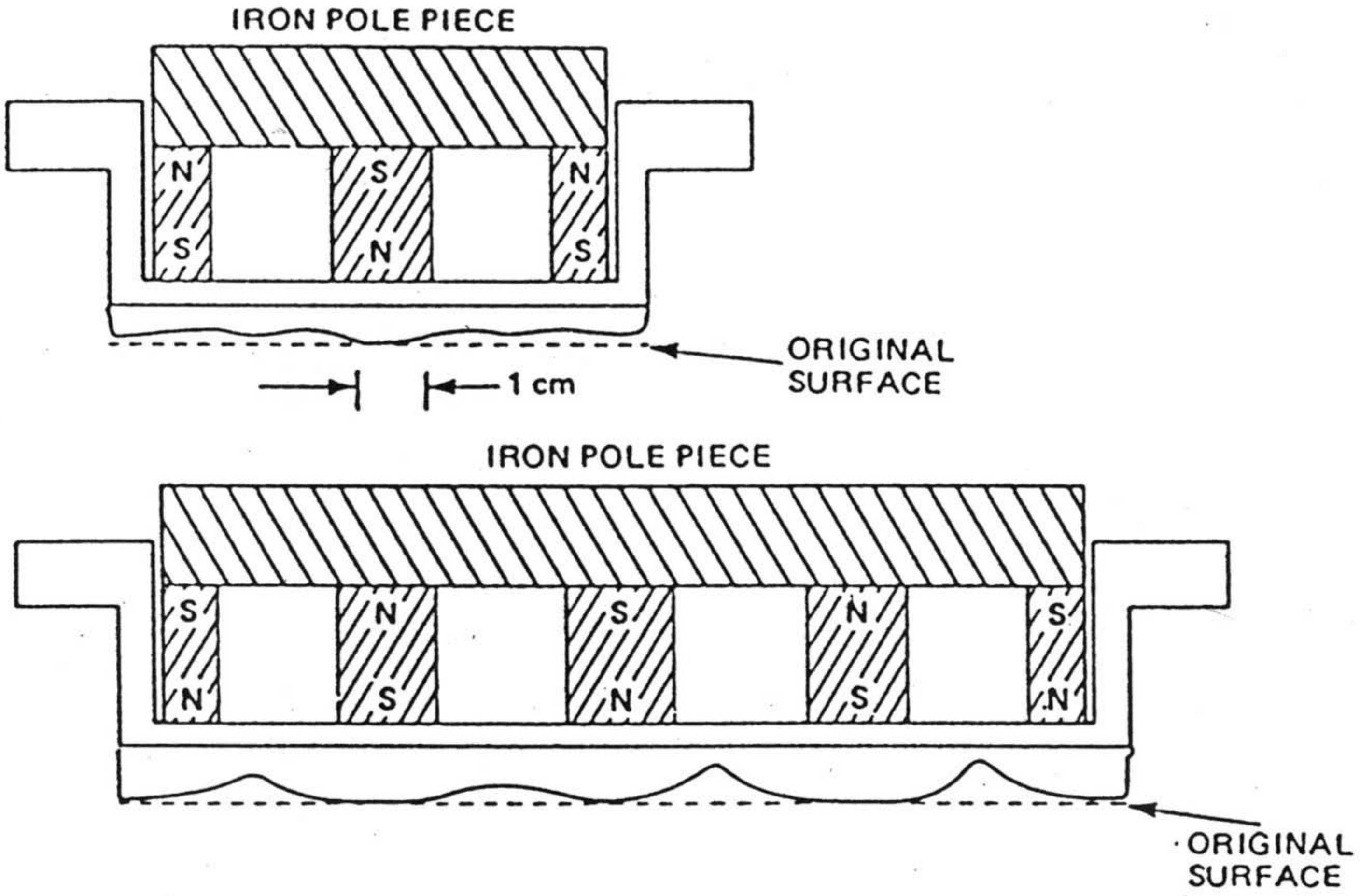

Repetition: I/V Characteristics

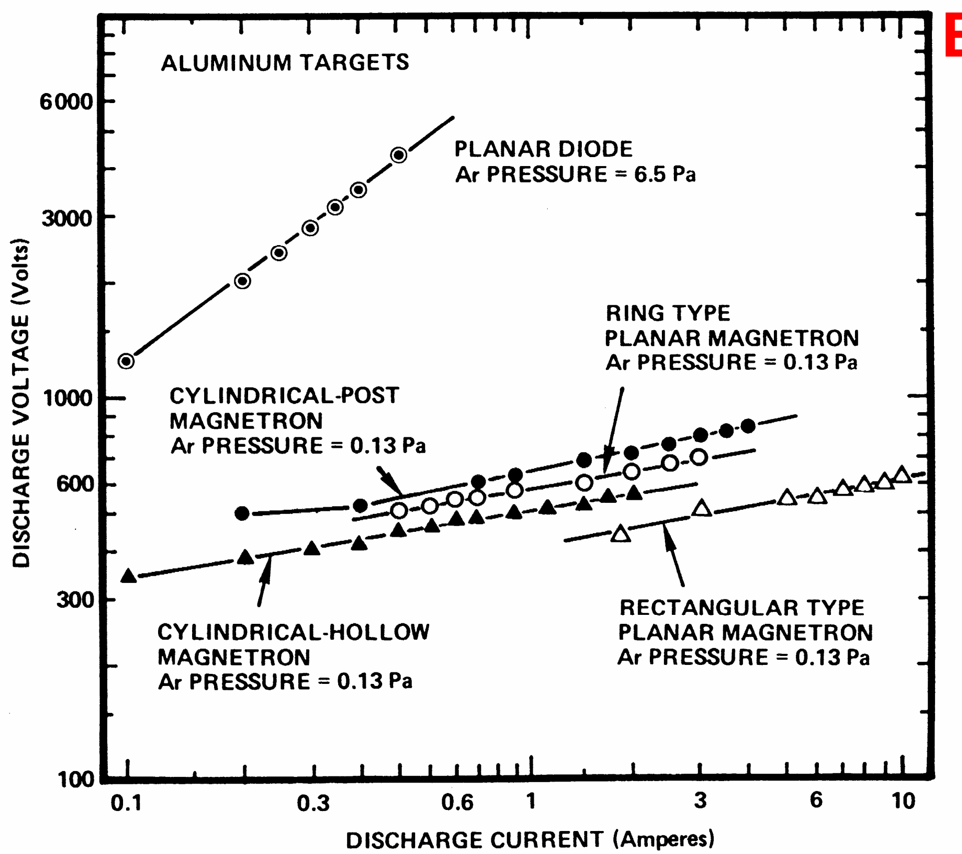

Empirical correlation:

$$R \propto I(k \cdot \ln U)$$

R = Erosion rate

I = Discharge current

U = Discharge voltage

Magnetron discharges work at significantly lower gas pressures!

Sputter Yield I

$$Y = \frac{\langle n \rangle}{n^+}$$

<n> = mean number of particles emitted per impingement
n^+ = number of impinging ions

Y is dependent on several parameters of the ions and of the target material.

Sputter Yield II

Dependence on :

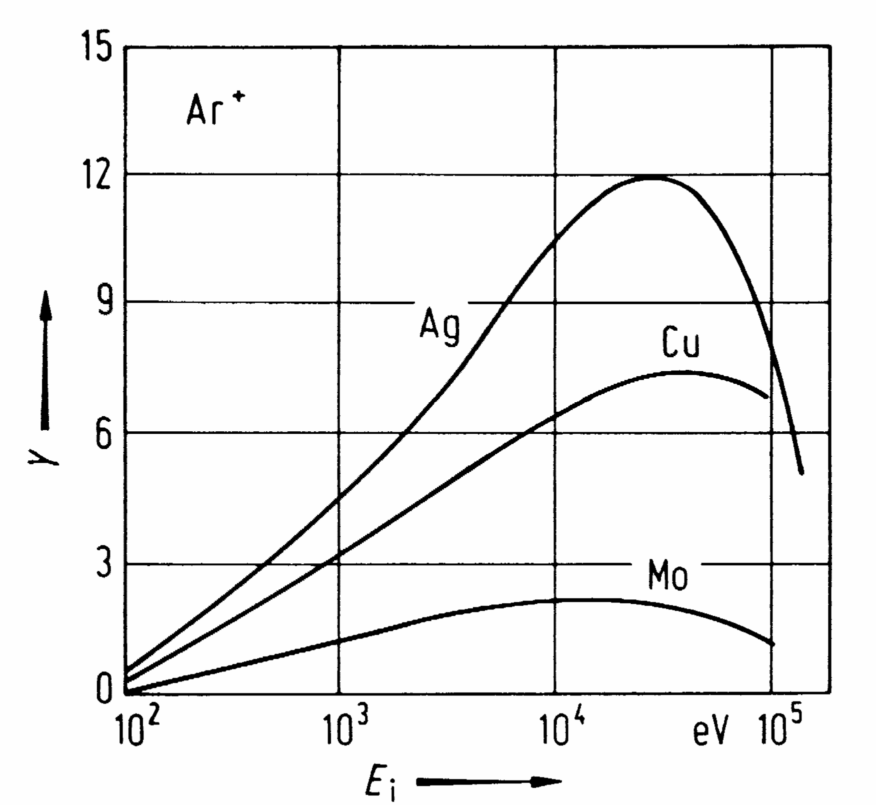

Ion energy

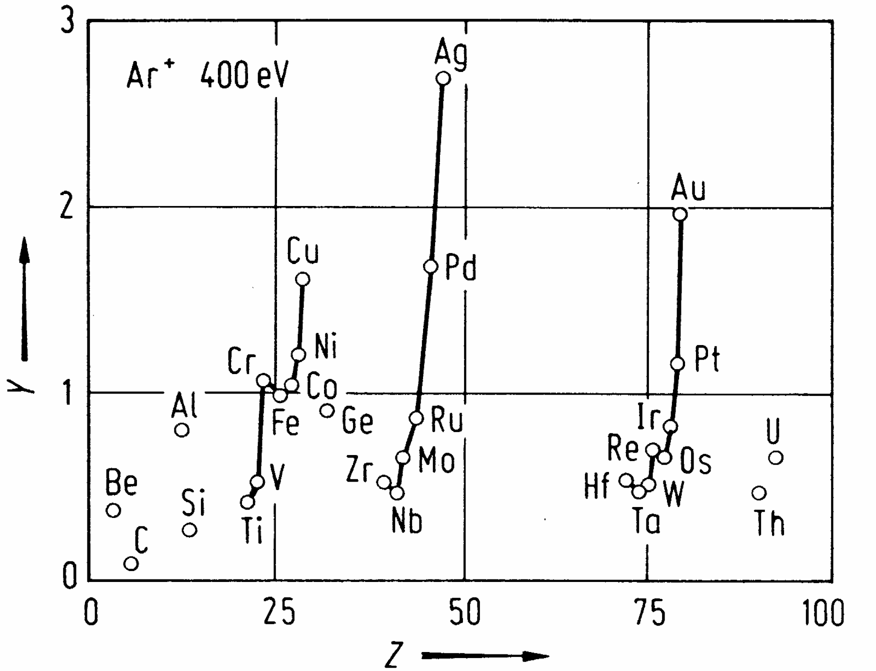

Target material

Sputter Yield III

Dependence on:

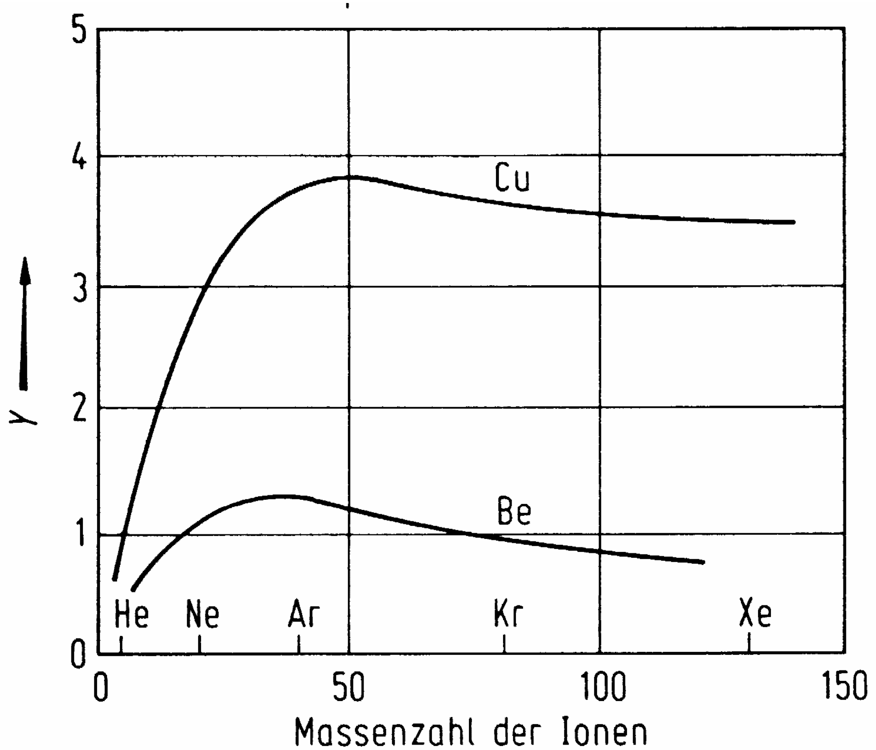

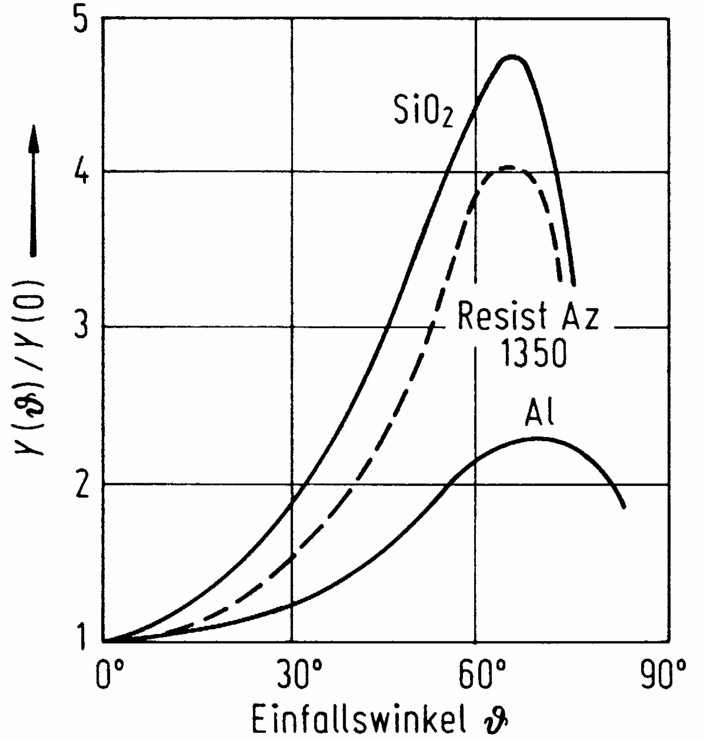

Ion mass **Ion impingement angle**

Sputtering Regimes: Single Knock On

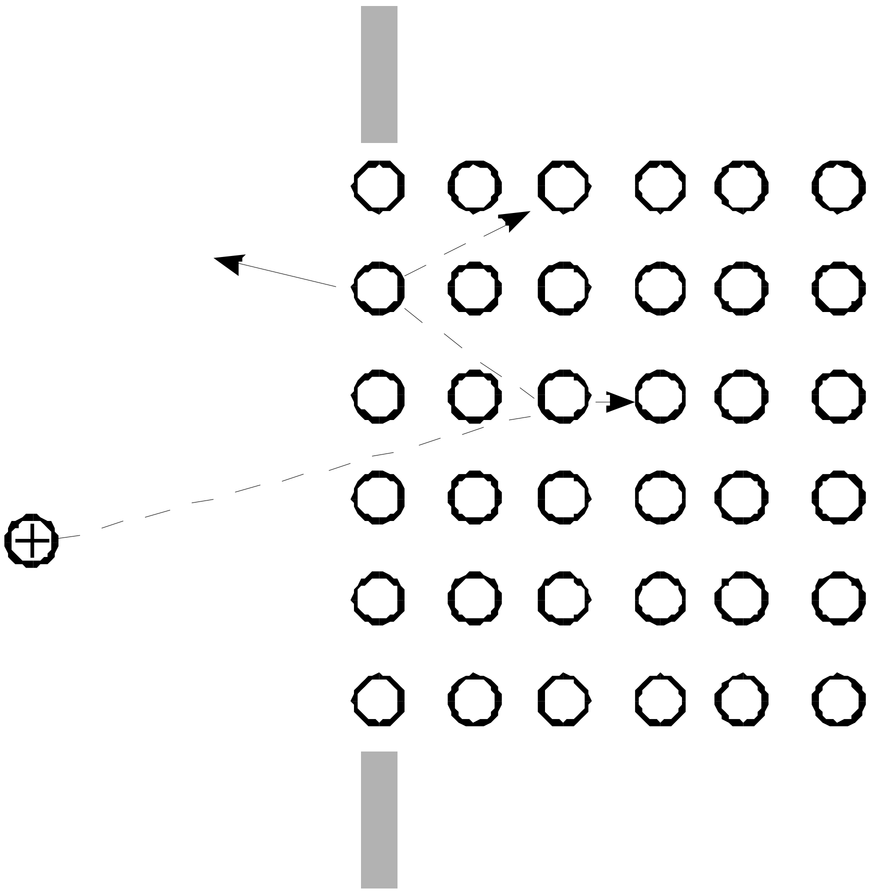

Ion energy small,
and/or
ion mass small

$$M^{+} <: Y \propto 10^{-1}$$

$$E^{+} < 10\text{eV}: Y \propto \frac{E^{+}}{U_0}$$

U_0 = Surface binding energy

Sputtering Regimes: Linear Collision Cascade I

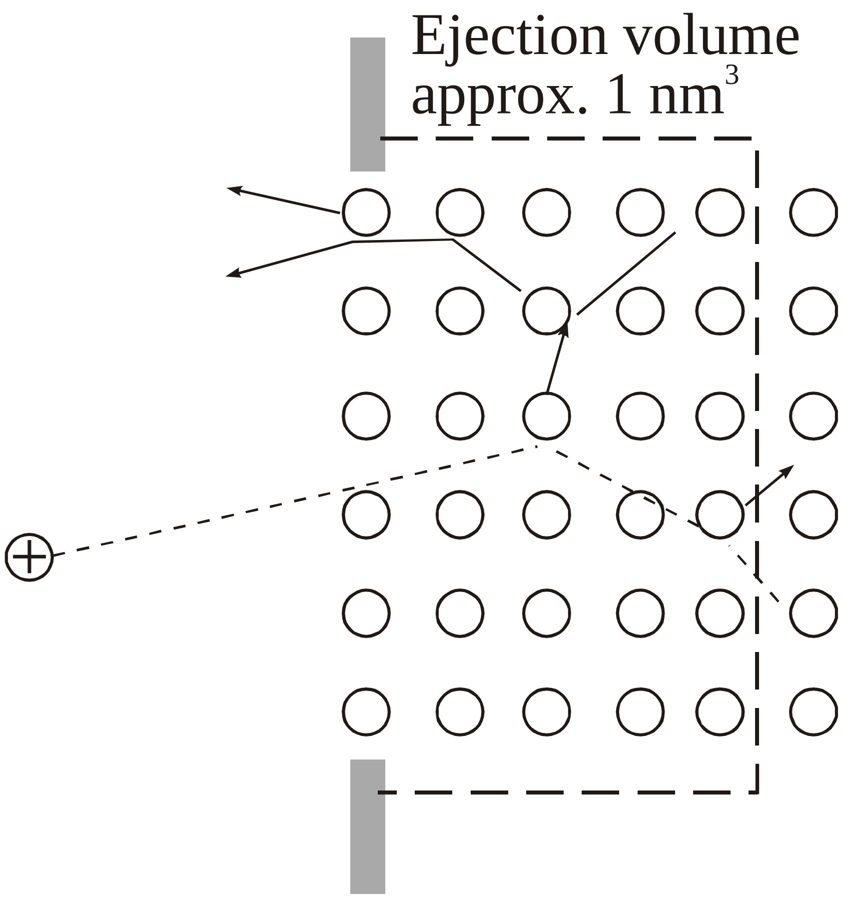

Ion energy: 0.1 - 10 keV

Collision potentials:

E^+ 0.1 - 1 keV: Born-Mayer

E^+ 1 - 10 keV: Thomas-Fermi

$$Y \propto \frac{4M^+ M_t}{\left(M^+ + M_t\right)^2} \frac{E^+}{U_0}$$

M_t = Mass of target atoms

Sputtering Regimes: Linear Collision Cascade II

Perpendicular impingement:

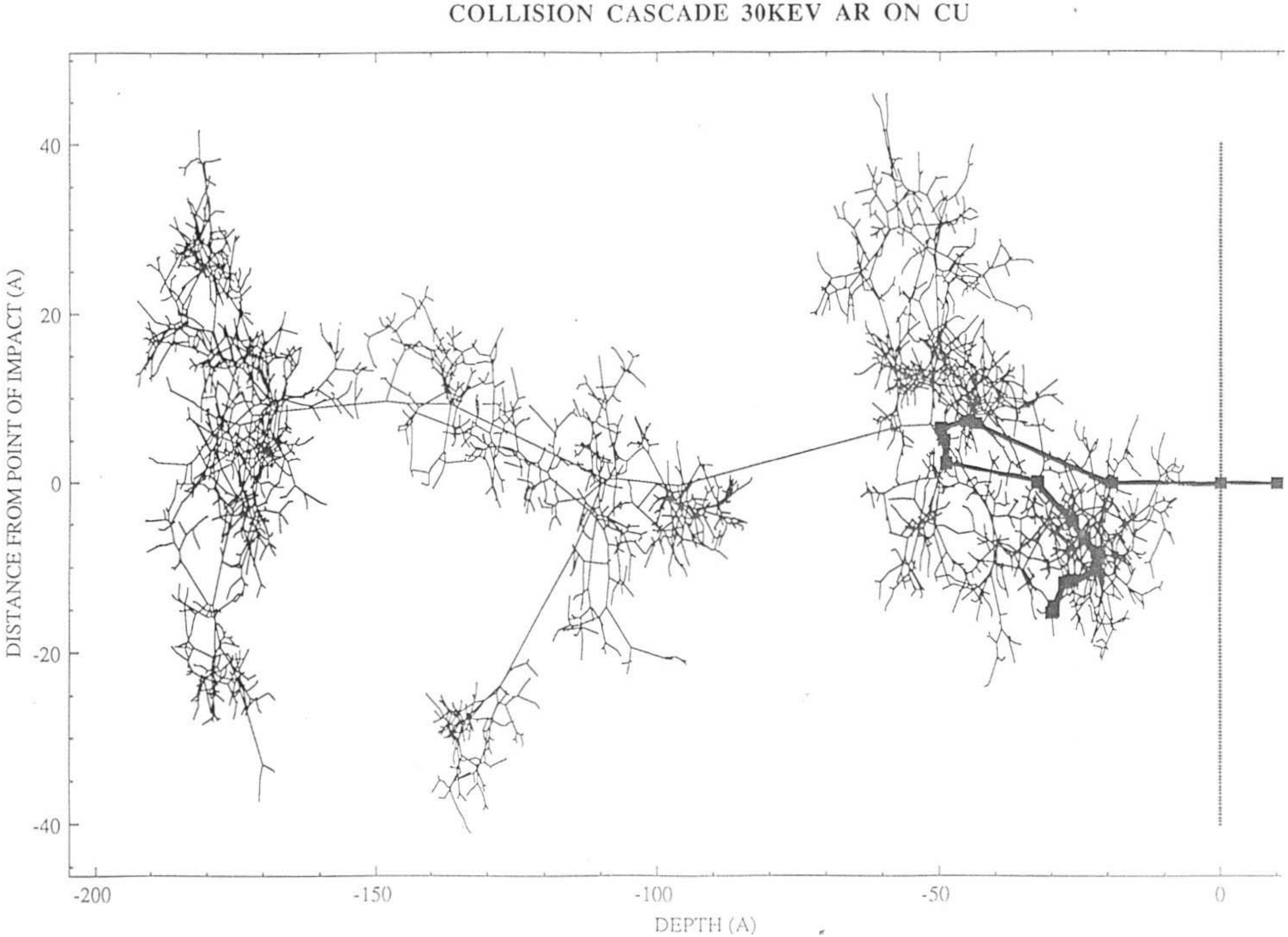

Sputtering Regimes: Linear Collision Cascade III

Oblique impingement:

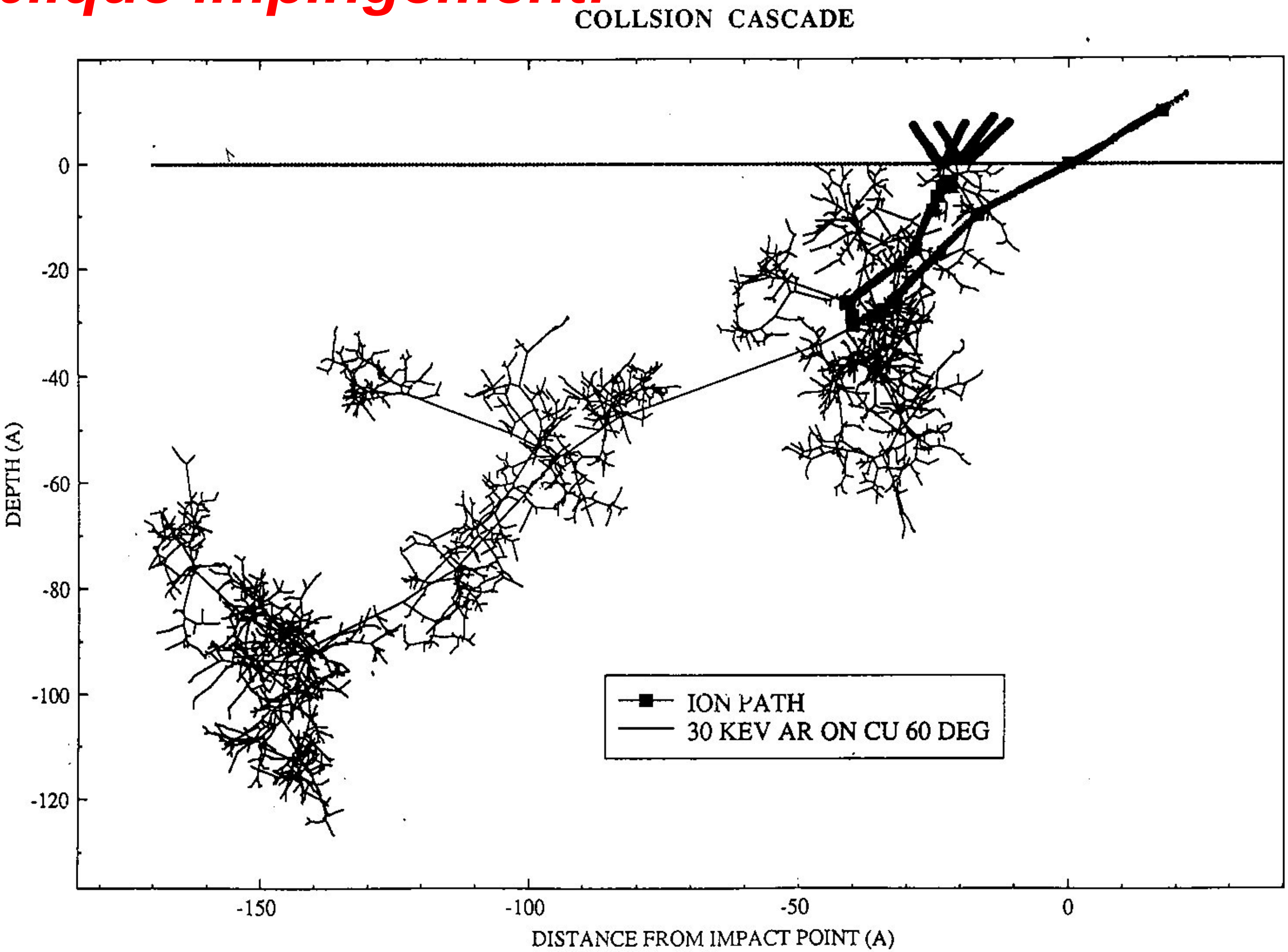

Sputtering Regimes: Thermal Spike

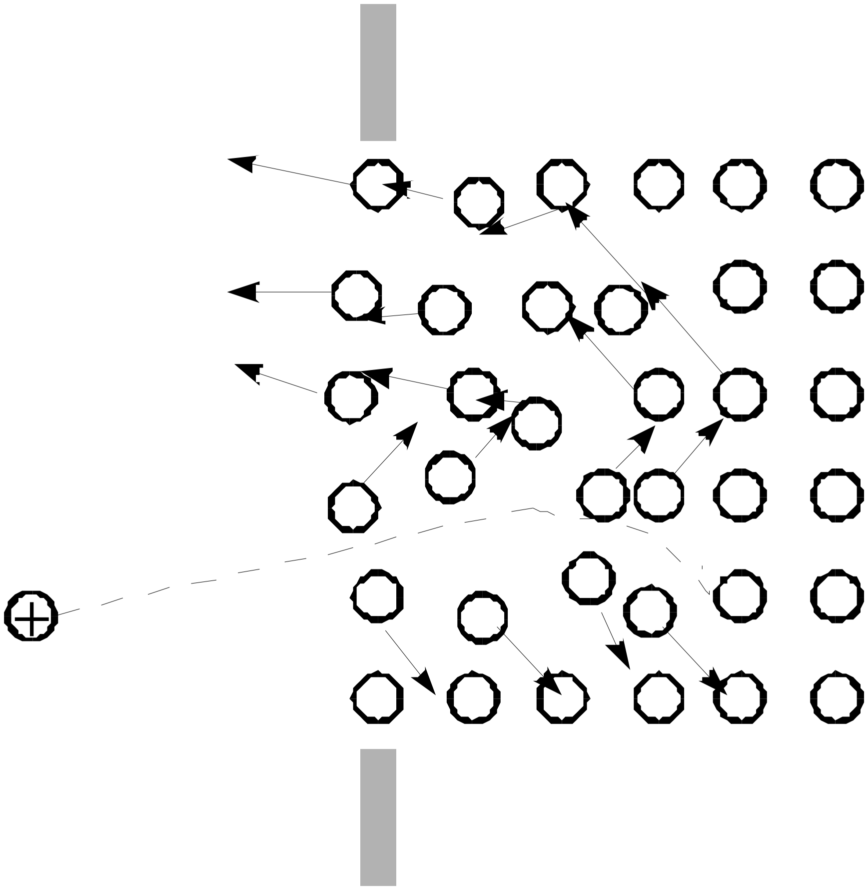

Ion energy > 10 keV

$$Y \propto \exp\left(-\frac{U_0}{k_B T}\right)$$

i. e. an evaporation-characteristic of the ejection volume

Linear Collision Cascade: Global Characteristics

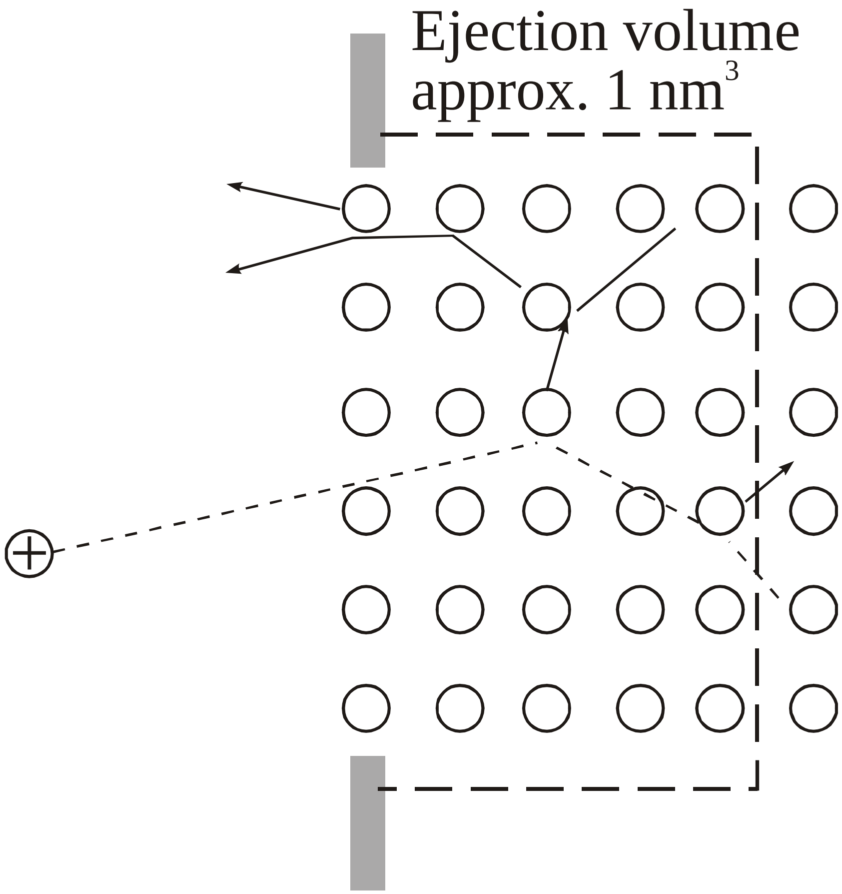

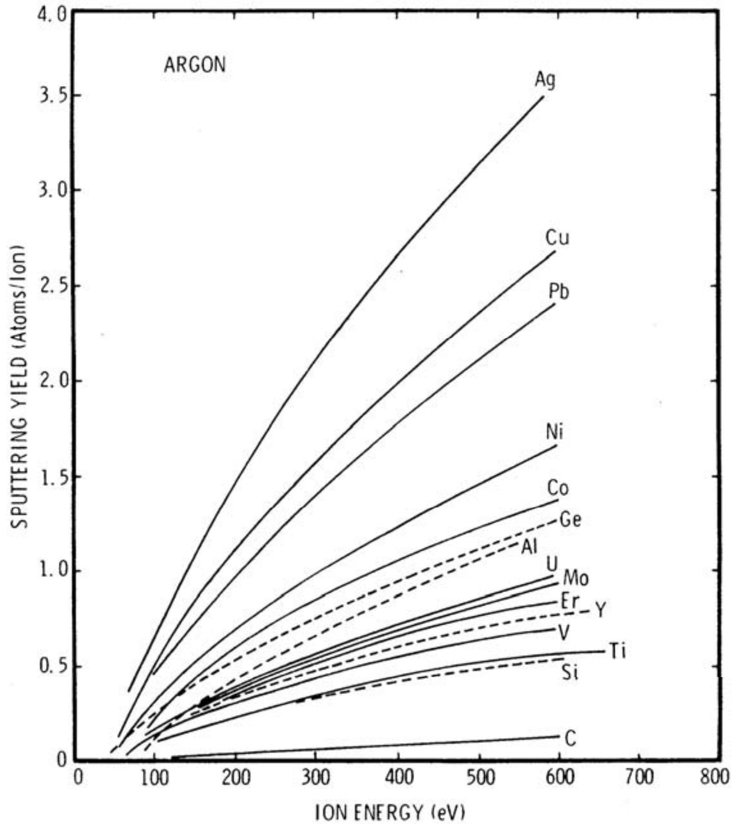

Y = 0,5 - 4

Sputtering Regimes: Simulation

www.srim.org

Stopping Range of Ions in Matter

Energy Distribution of Ejected Particles

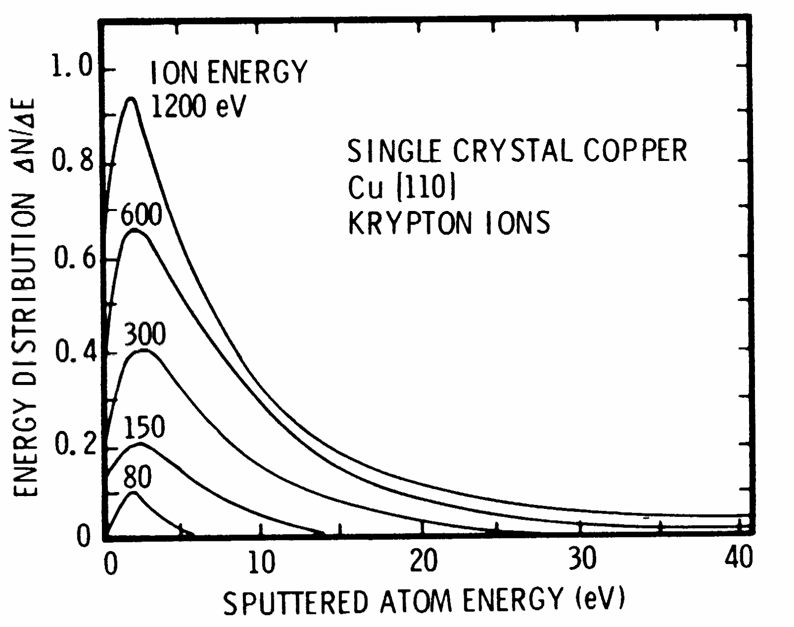

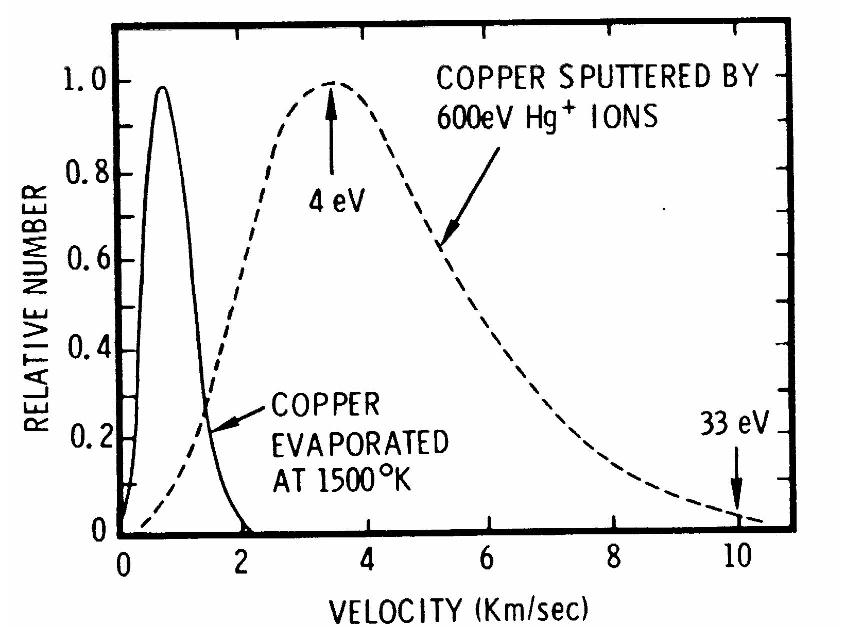

The energy distribution of sputtered particles is significantly different from that of thermally evaporated ones.

Linear Collision Cascade: Energy Distribution

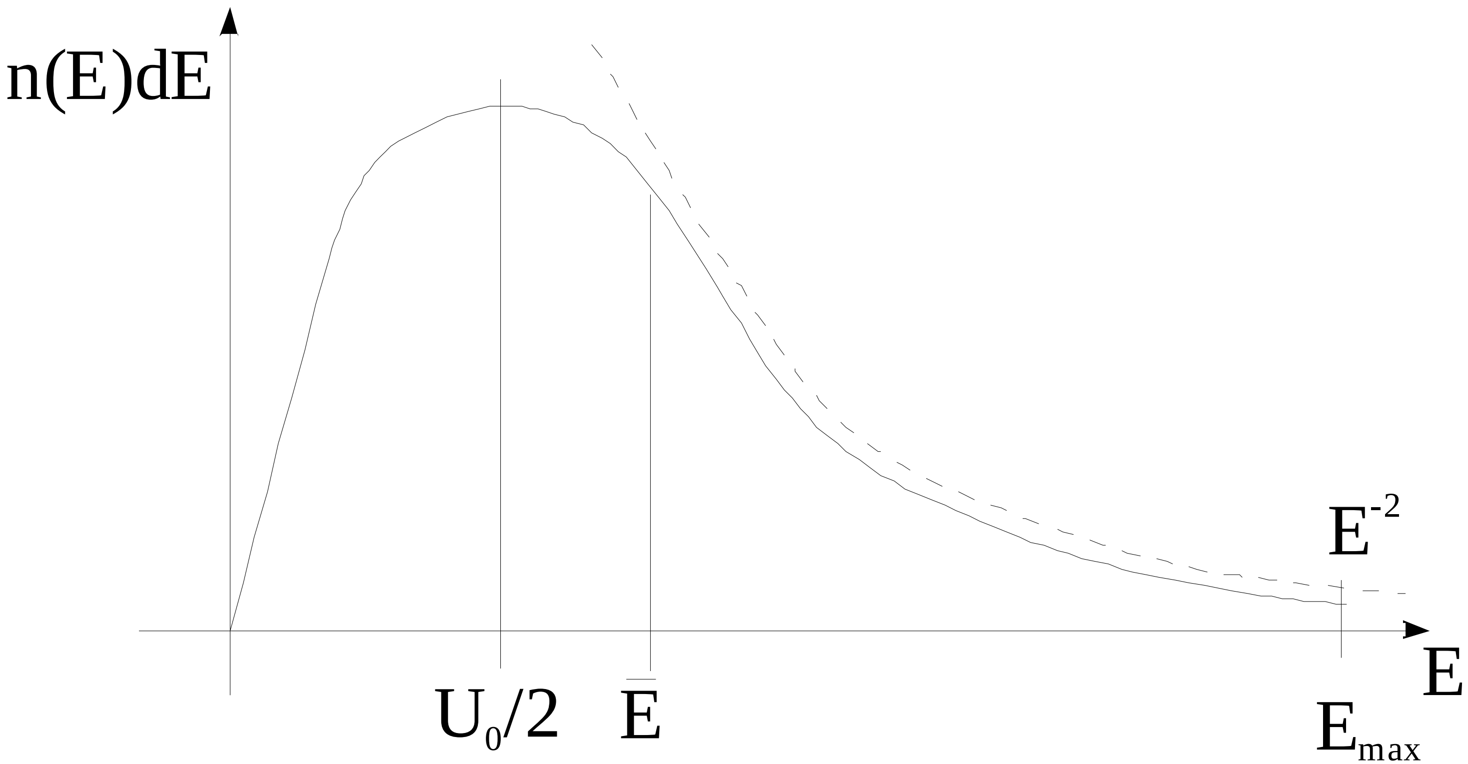

$$n(E)dE \propto \frac{E}{(E+U_0)^3}\,dE$$

E_{max} = maximum energy, $E_{max} \propto E^{+}$

$\bar{E}$ = mean emission energy

Linear Collision Cascade: Angular Distribution

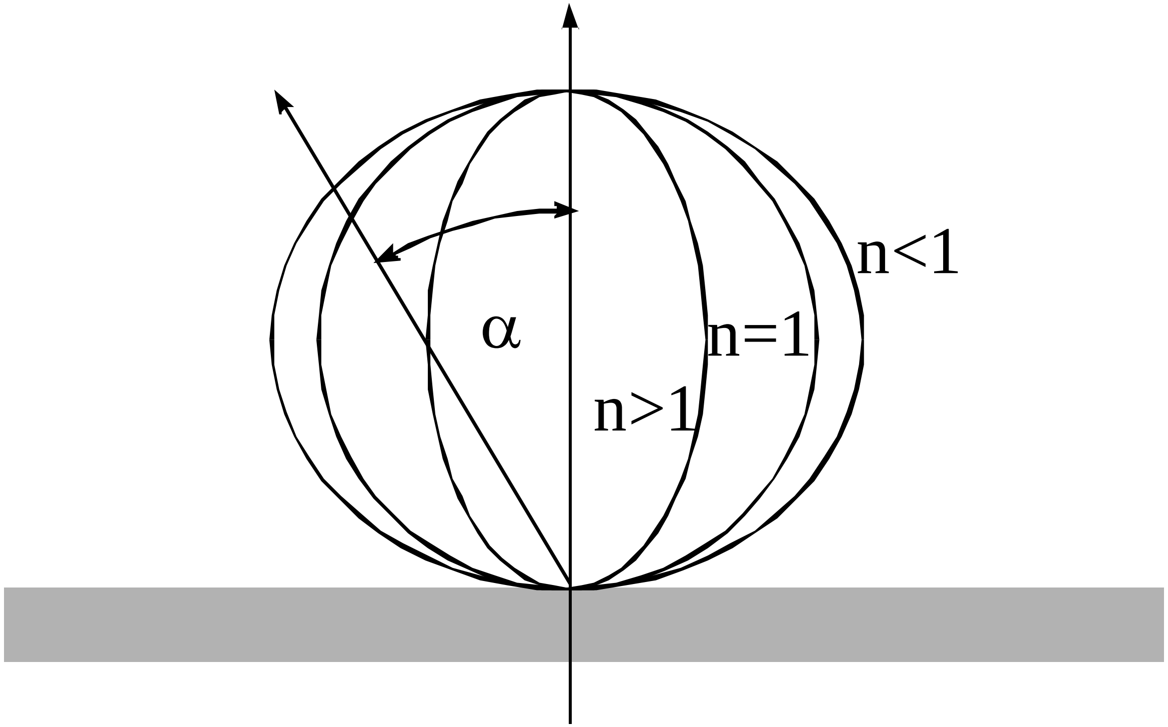

$$n(\alpha) \propto \cos^n \alpha$$

$n \leq 1$ E < 1 keV

$n > 1$ E > 1 keV

Sputtering of Alloys: Different Y

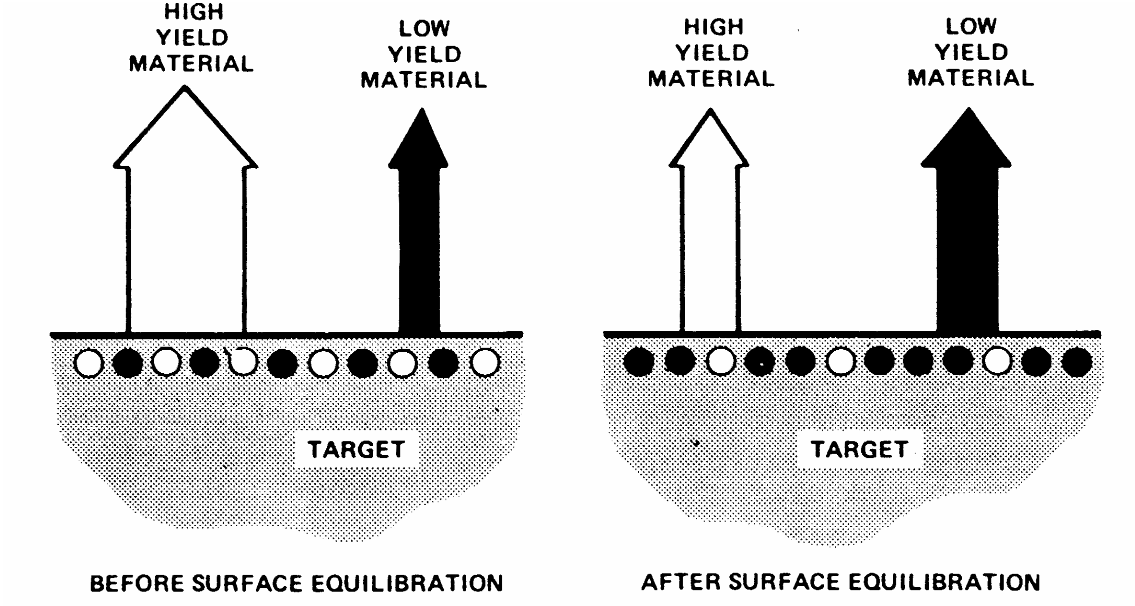

In the case of the homogenous distribution of the constituents the vapor composition is (after a transient regime) identical to the target composition.

Sputtering of Alloys: Cone Formation I

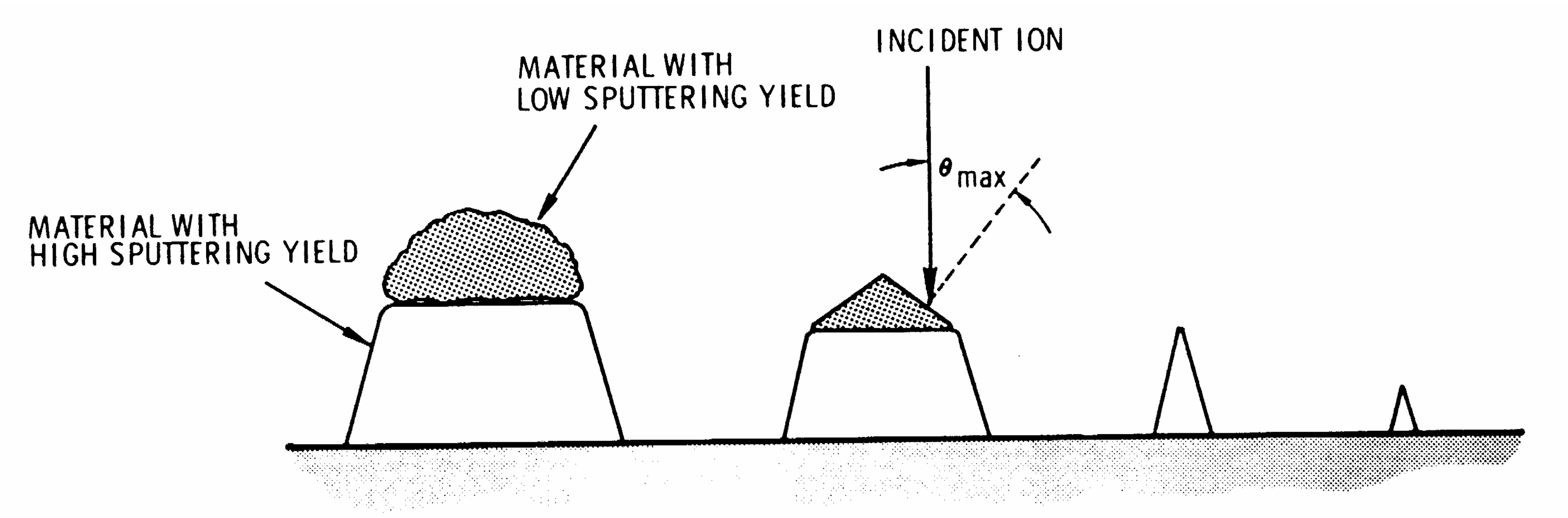

If a low yield material is present in the form of macroscopic preciptates, cones can be formed on the target surface.

Sputtering of Alloys: Cone Formation II

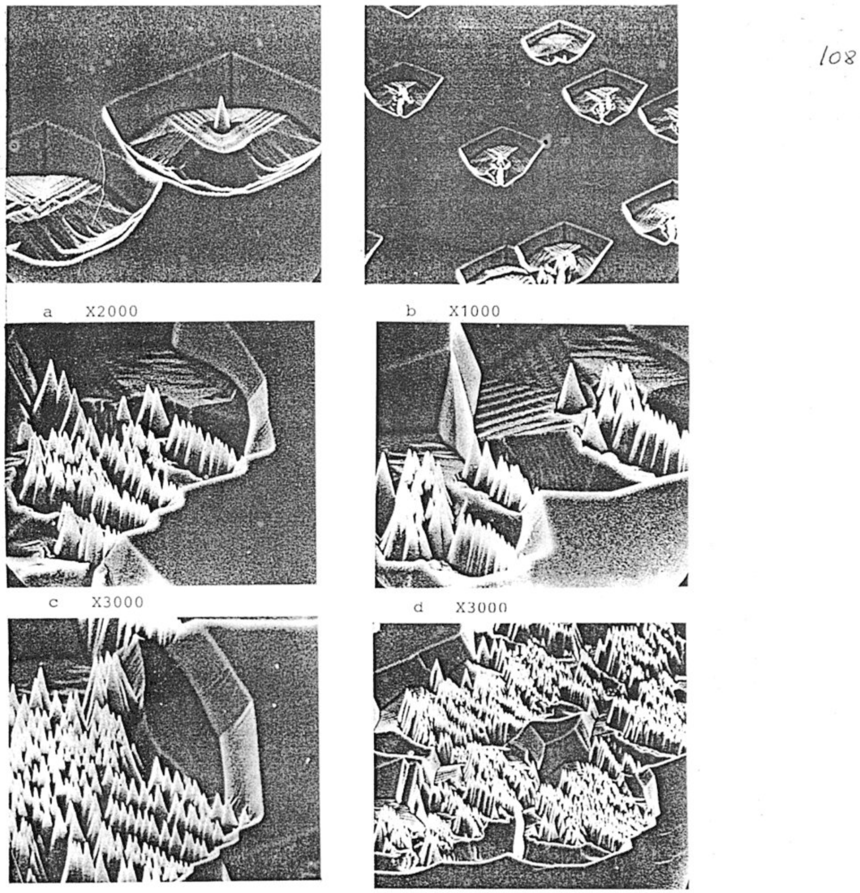

(11 3 1) Cu nach Fluence : $1 \cdot 10^{19} \cdot 40 keV Ar^{+} \cdot cm^{-2}$

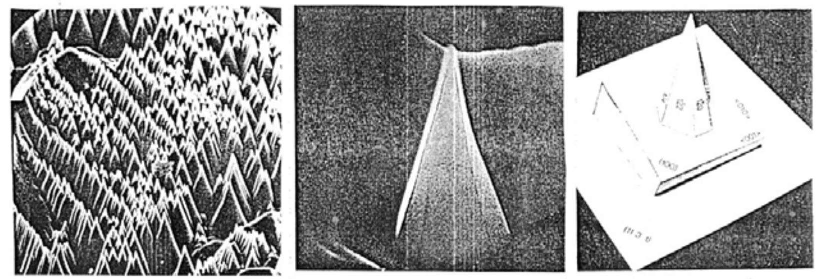

Fig. 4a X2000

Fig. 4b X20,000

(11 3 1) Einkristall Cu, 10^{19} 40keV Ar^{+} cm^{-2}

Pyramide

The terminating surfaces of the cones are often low index crystal planes or have an inclination corresponding to surfaces with maximum sputter yield.

Sputtering of Single Crystals: Channelling

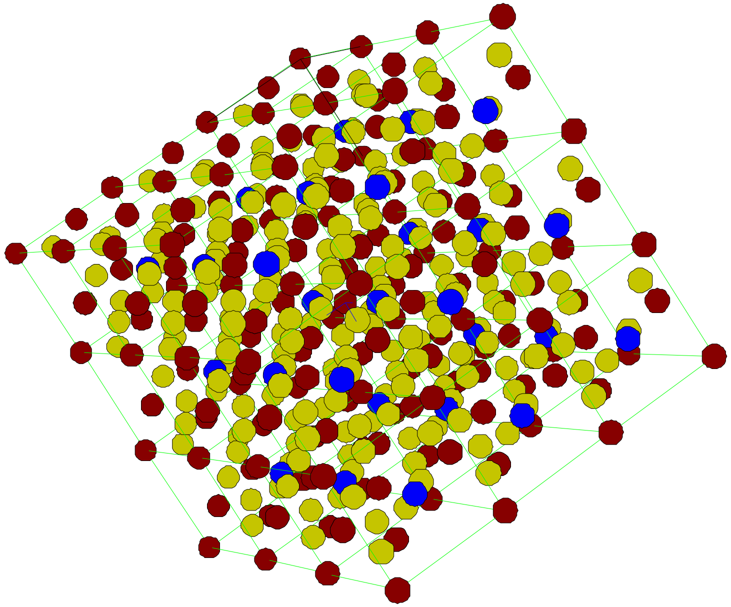

Ions may penetrate a single crystal more or less deep in dependence on their impingement direction.

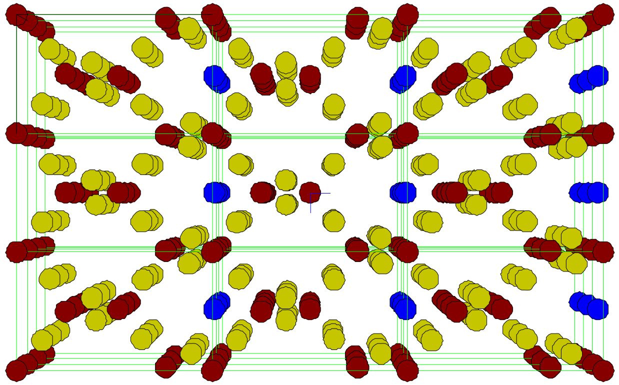

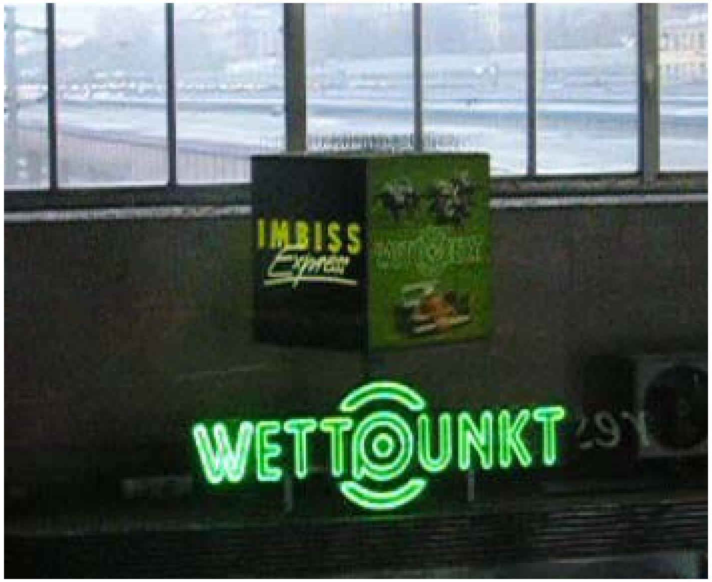

Sputtering of Single Crystals: Wehner-Spots

Focusing of the impulse along densly packed crystallographic directions:

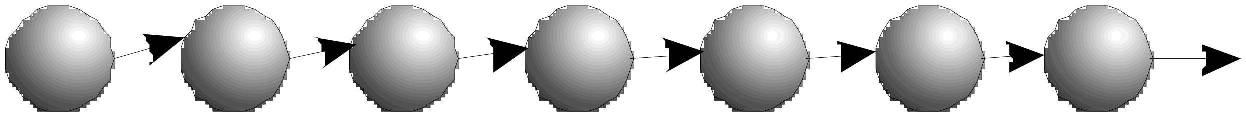

Y = maximum along these directions! If a hemispherical collector is placed above the target, one can detect the so-called "Wehner Spots".

Reactive Processes I

In the case of reactive sputtering processes compounds of the sputtered material and the reactive gas are formed at the target and the substrate.

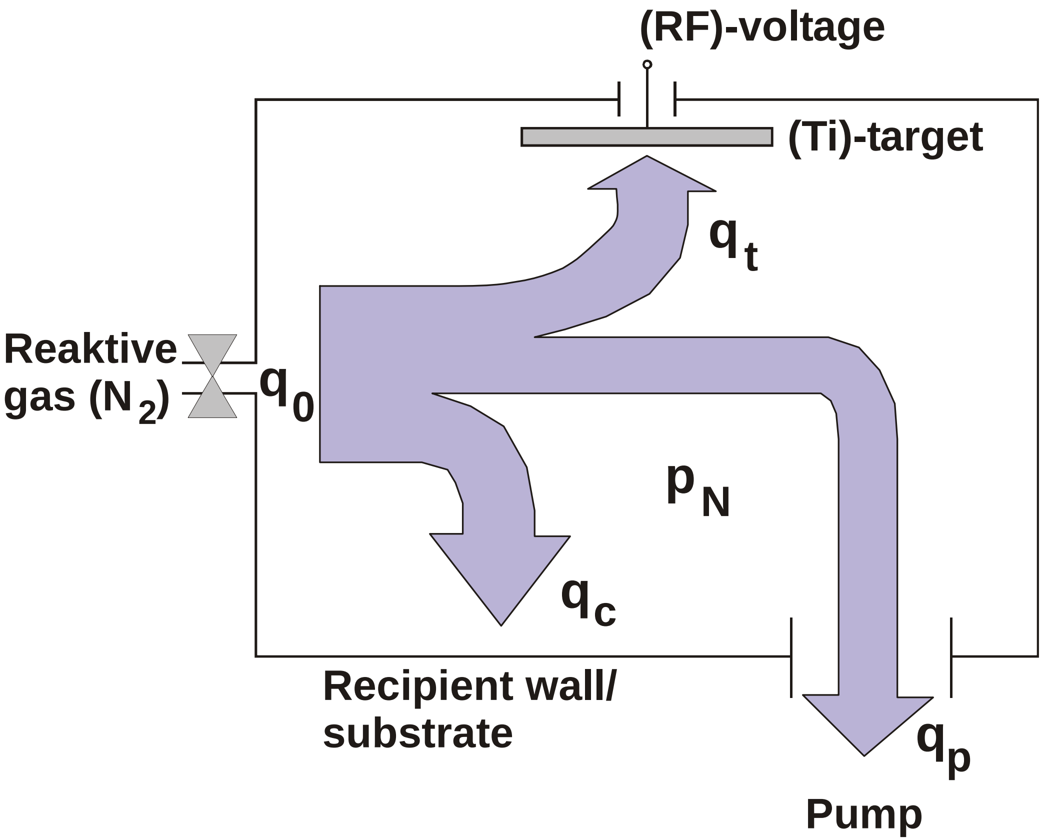

Berg-model

Gas flows of the reactive gas, q_i:

$$q_0 = q_t + q_c + q_p$$

q_0 ... Total flow
q_t ... Flow to target
q_c ... Flow to wall
q_p ... Flow to pump

Reactive Processes II

Balance of areal coverages and particle flows:

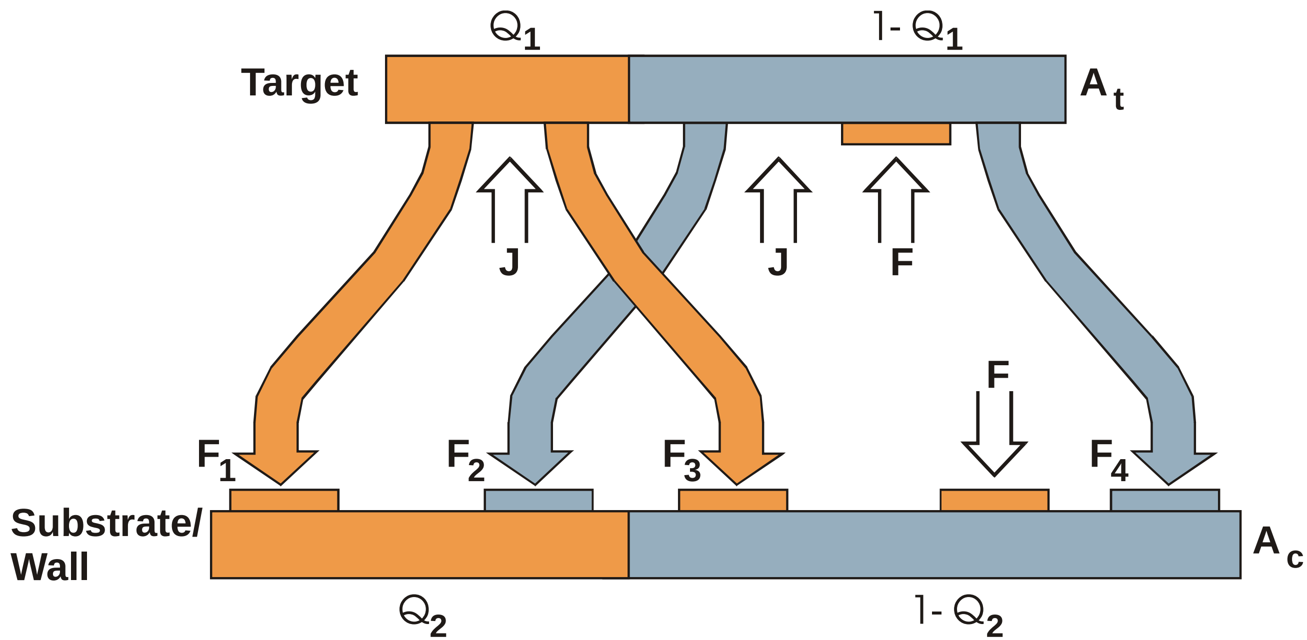

Θ_1 ... Reacted surface target

Θ_2 ... Reacted surface Wall

$F_{1,3}$ ... Flows of reaction product

$F_{2,4}$ ... Flows of metal particles

J ... Flow of workong gas

F ... Flow of reactive gas

Result: system of numerically solvable balance equations

Reactive Processes: Example TiN I

Erosion rate at the target in dependence on the N_2-flow:

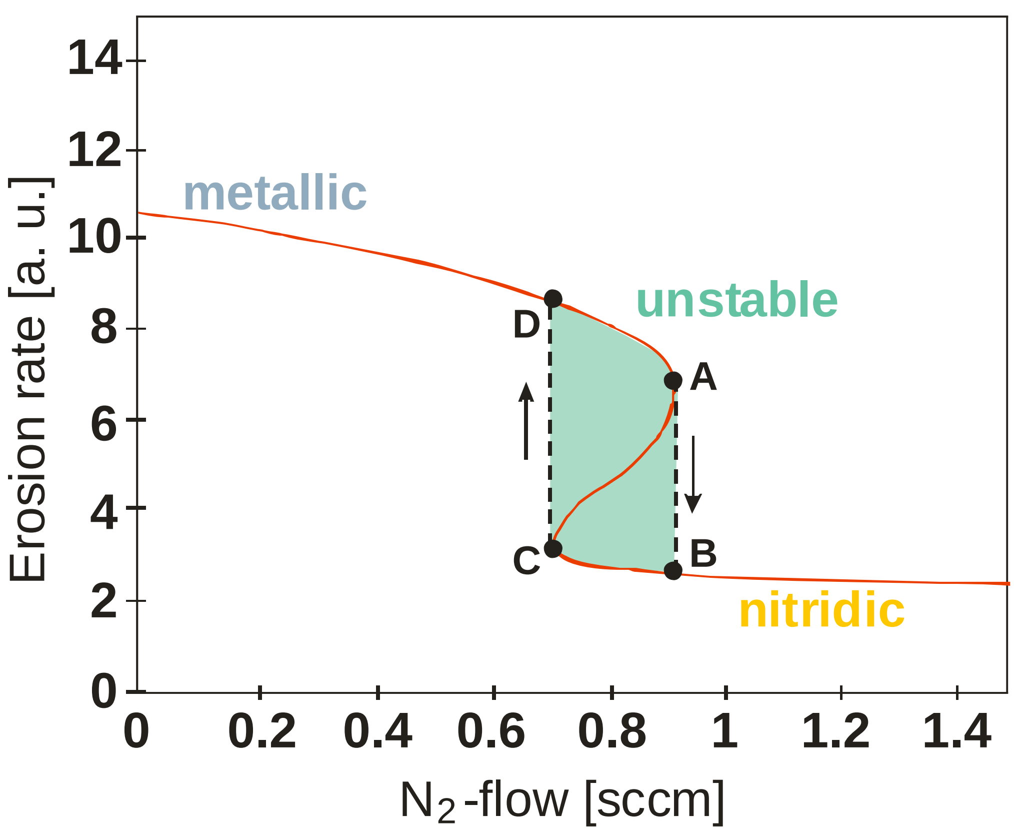

Hysteresis at the transition from the metallic to the nitridic mode.

Reactive Processes: Example TiN II

Pressure in the chamber in dependence on the N_2- flow:

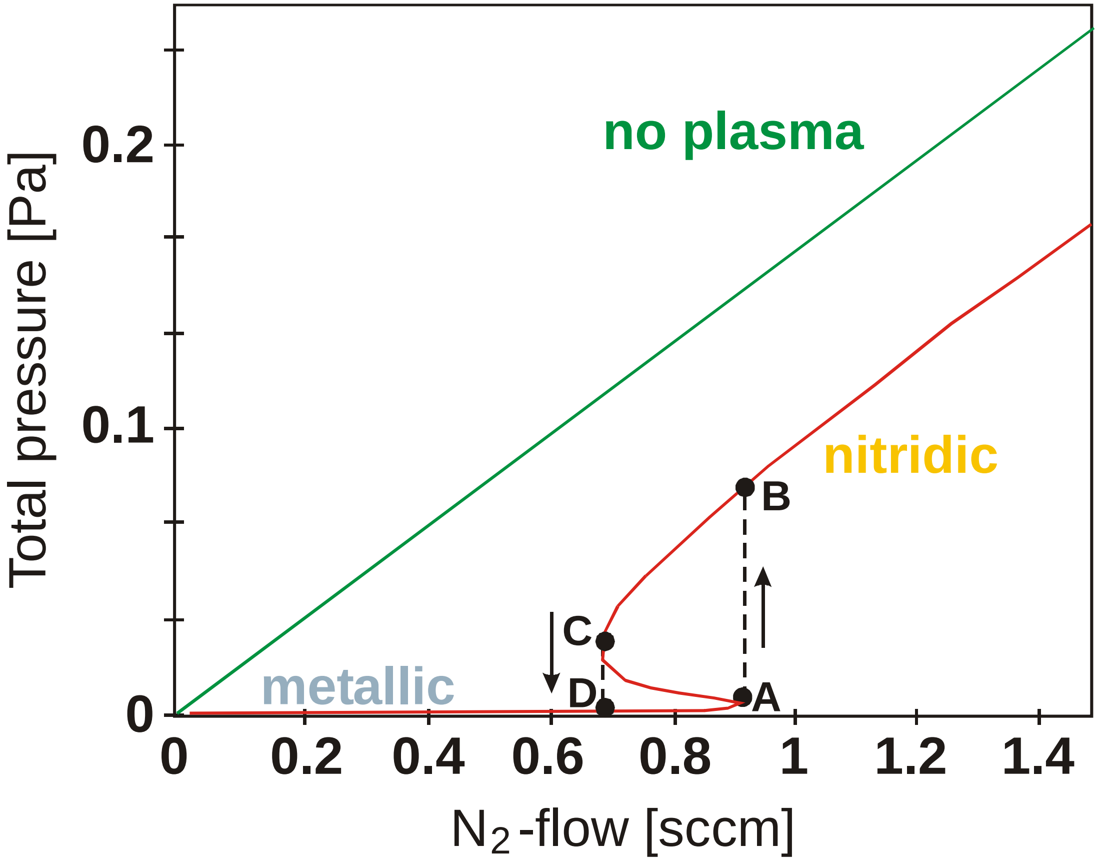

At first all N_2 is consumed; the unstable operating point A would be the optimum working condition

TiN: Experimental Data

The hysteresis in the relation betweem N_2-flow and total pressure is well visible.

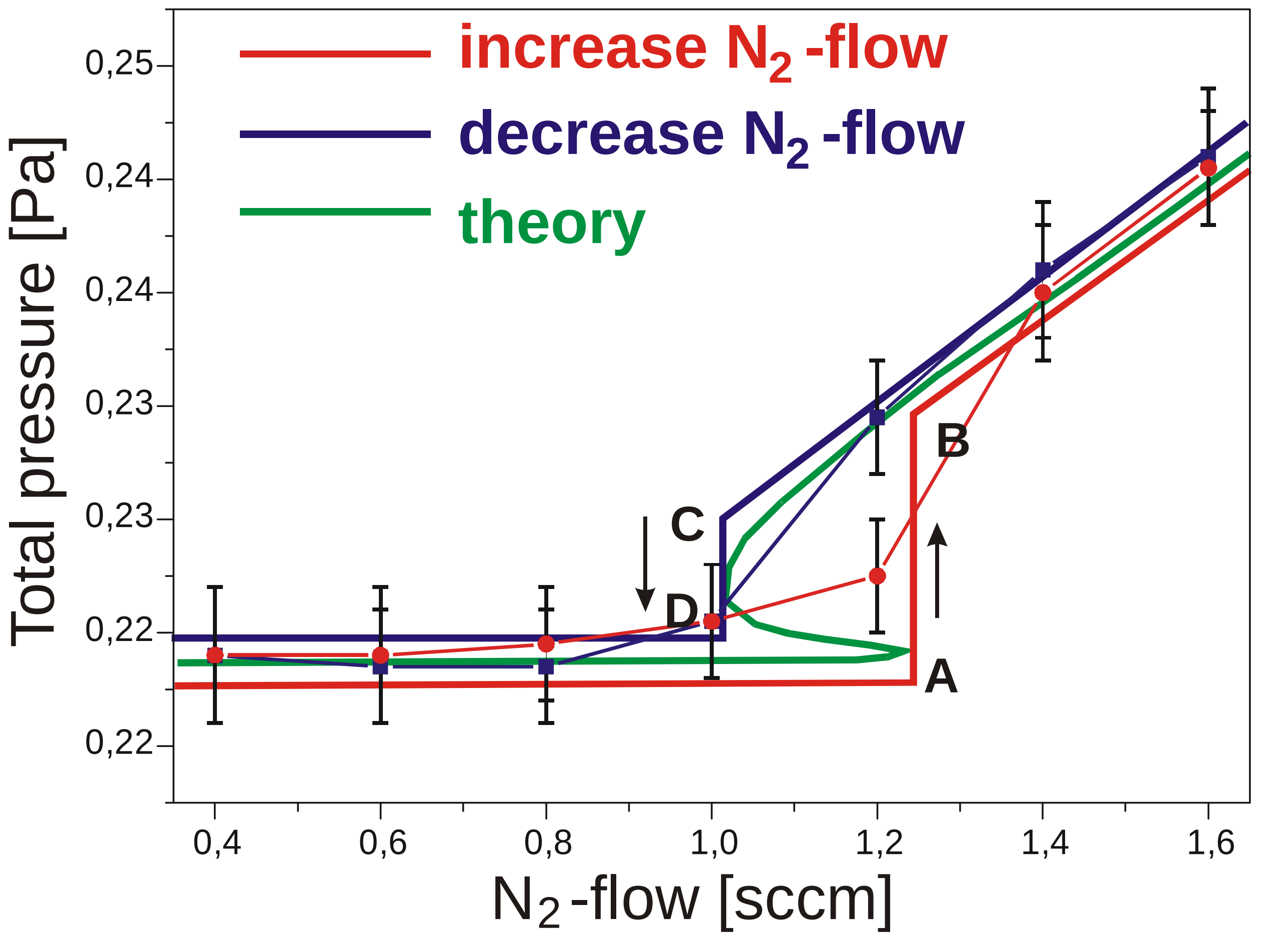

Reactive Processes: Large Plants

Sputtering plant for the reactive deposition of solar cell materials.

Reactive sputtering processes have recently been accepted as suitable methods for the deposition of oxidic, nitridic and carbidic materials.